J|A|C|S ARTICLES

Published on Web 11/22/2010

Ca_2LiC_3H: A New Complex Carbide Hydride Phase Grown in Metal Flux

David A. Lang,[†] Julia V. Zaikina,[†] Derek D. Lovingood,[‡] Thomas E. Gedris,[†] and Susan E. Latturner*,[†]

Department of Chemistry and Biochemistry, Florida State University, Tallahassee, Florida 32306, United States, and Department of Chemistry, Valdosta State University, Valdosta, Georgia 31698, United States

Received August 17, 2010; E-mail: latturne@chem.fsu.edu

Abstract: The reaction of carbon and CaH_2 in a calcium/lithium flux mixture produces crystals of the new compound Ca_2LiC_3H. This phase forms with a new structure type in tetragonal space group *P4/mbm* (a = 6.8236(1) Å, c = 3.7518(1) Å, Z = 2, R_1 = 0.0151). This is a stuffed variant of the $Cs_2(NH_2)N_3$ structure, containing hydride anions in octahedral sites; the structure determination by single-crystal X-ray diffraction surprisingly allowed the hydrogen to be detected. The Ca_2LiC_3H structure also features the rarely seen C_3^{4-} carbide anion; the protolysis reaction of this compound with ammonium chloride produces C_3H_4. The electronic properties of Ca_2LiC_3H were studied by quantum-chemical calculations including band structure and electron localization function (ELF) analysis; the phase is a charge-balanced semiconductor with a calculated band gap of 0.48 eV. This is in agreement with ^{7}Li, ^{13}C, and ^{1}H MAS NMR data, which show resonances in the ionic region instead of the Knight shifted region. ELF analysis of the theoretical nonhydrided Ca_2LiC_3 structure confirms the ability of these calculations to properly locate hydrides and supports the structural model based on X-ray diffraction data.

Introduction

Synthesis in metal fluxes has proven to be a versatile method for the discovery of new intermetallic and Zintl phases, as well as for formation of large crystals of known metastable or peritectic compounds.[1] We have been investigating the use of mixed fluxes, which allow for the solvation of a wide range of reactants and lowered reaction temperatures due to formation of eutectics. For instance, the La/Ni eutectic is a fruitful solvent for growth of intermetallics with interesting magnetic properties and complex structures such as $La_{21}Fe_8Sn_7C_{12}$ and $LaRu_2Al_2B$.[2] Flux mixtures of Mg and Al promote crystallization of lightweight compounds such as CaMgSi, which may be of interest in aerospace alloys or for hydrogen storage applications.[3] We are continuing our work on synthesis in light metal fluxes by investigating lithium-containing mixtures.

All mixtures of lithium and calcium with greater than 50 at. % lithium melt below 573 K.[4] In addition to dissolving many metals, Ca/Li flux solvates lightweight refractory elements such as carbon and boron. It also dissolves many ionic compounds such as CaH_2, Ca_3N_2, and LiF. This allows for synthesis of phases ranging from strongly delocalized intermetallics to complex salts. In particular, dissolution of CaH_2 makes Ca/Li flux a very promising medium for growth of new metal hydride phases, which are of great recent interest as hydrogen storage materials. Metal hydrides include intermetallic hydrides with variable content of chemisorbed hydride interstitials (e.g., $LaNi_5H_x$, where x can vary from 0 to 6); ionic hydrides such as NaH or CaH_2 or more complex charge-balanced Zintl phase hydrides with covalently bound or anionic hydrogen; and phases containing covalent metallohydride species such as $LiBH_4$ or $NaAlH_4$.[5] In addition to their potential hydrogen storage capabilities, these compounds often lie on the border between complex salts, classical Zintl phases, and intermetallics and feature interesting structural characteristics.

The reaction of carbon and CaH_2 in Ca/Li flux produces Ca_2LiC_3H, which has a new structure incorporating both the rare C_3^{4-} carbide anion and a clearly defined hydride anion. Metal carbides are a relatively sparsely investigated class of compounds, with Jeitschko and Pöttgen responsible for much of the recent discoveries of new phases.[6,7] Most metal carbides feature monatomic carbide anions (C^{4-}), with acetylide anions (C_2^{2-}) being much less common and more complex carbide anions such as C_3^{4-} rarer still. The C_3^{4-} anion can be viewed as deprotonated allene. This allenylide anion, first definitively observed in Sc_3C_4, is also found in Mg_2C_3, but the calcium

[†] Florida State University.
[‡] Valdosta State University.

(1) Kanatzidis, M. G.; Pöttgen, R.; Jeitschko, W. *Angew. Chem., Int. Ed.* **2005**, *44*, 6996–7023.
(2) (a) Benbow, E. M.; Dalal, N.; Latturner, S. E. *J. Am. Chem. Soc.* **2009**, *131*, 3349–3354. (b) Zaikina, J. V.; Jo, Y. J.; Latturner, S. E. *Inorg. Chem.* **2010**, *49*, 2773–2781.
(3) Whalen, J. B.; Zaikina, J. V.; Achey, R.; Stillwell, R.; Zhou, H.; Wiebe, C. R.; Latturner, S. E. *Chem. Mater.* **2010**, *22*, 1846–1853.
(4) Massalski, T. B.; Okamoto, H. *Binary Alloy Phase Diagrams*, 2nd ed.; ASM International: Materials Park, OH, 1990.
(5) Häussermann, U. *Z. Kristallogr.* **2008**, *223*, 628–635.
(6) Pöttgen, R.; Jeitschko, W. *Inorg. Chem.* **1991**, *30*, 427–431.
(7) (a) Dashjav, E.; Kreiner, G.; Schnelle, W.; Wagner, F. R.; Kniep, R.; Jeitschko, W. *J. Solid State Chem.* **2007**, *180*, 636–653, and references therein. (b) Musanke, U. E.; Jeitschko, W. *Z. Naturforsch.* **1991**, *46b*, 1177–1182. (c) Czekalla, R.; Hüfken, T.; Jeitschko, W.; Hoffmann, R. D.; Pöttgen, R. *J. Solid State Chem.* **1997**, *132*, 294–299. (d) Hoffmann, R. *Am. Sci.* **2002**, *90*, 318–320.

analogue of this phase does not exist.[6,8] The structure of Ca_2LiC_3H may be stabilized by a strong interaction between the hydride anion and neighboring lithium cations, which is evidenced by observed bond lengths, density of states and electron localization function calculations, and ^1H NMR data. With the unprecedented coexistence of the C_3^{4-} and H^- anions, Ca_2LiC_3H represents a new lightweight complex salt, and the first ordered metal carbide hydride.

Experimental Section

Synthesis. Reactants were used as received: calcium shot (99.5% Alfa Aesar), lithium rod (99.8% Strem Chemicals), acetylene carbon black (99.9% Strem Chemicals), and calcium hydride (98%, Alfa Aesar). Ca/Li/C/CaH_2 mmol ratios of 10:10:(1−9):(0−1) produced the desired product, with the highest yield produced using a ratio of 10:10:6:1. The reactants were weighed out in an argon-filled glovebox and placed into stainless steel crucibles (7.0 cm length/0.5 cm diameter). After the open ends of the crucibles were sealed by arc welding under argon, they were placed in silica tubes which were then sealed under vacuum. These ampules were heated to 1323 K in 2 h and were kept at this temperature for 2 h. They were cooled to 1073 K in 24 h, and then cooled to 773 K in 108 h. At 773 K, the tubes were removed from the furnace, inverted, and centrifuged to force the excess molten Ca/Li mixture off of the product crystals. Much of the crystalline product adheres to the surface of the steel crucible during growth and centrifugation, so use of a filter to separate the crystals from the flux is not necessary. Crucibles were cut open under an argon atmosphere in a glovebox. The solid product consists of silver reflective rectangular crystals, which oxidize within a few minutes of being exposed to air.

Elemental Analysis. Initial elemental analyses were performed using a JEOL 5900 scanning electron microscope with energy dispersive spectroscopy (SEM-EDS) capabilities. Samples were affixed to an aluminum SEM stub using carbon tape and analyzed using a 30 kV accelerating voltage and an accumulation time of 60 s. Because of considerable oxidation from brief contact with air during sample loading, the cleanest appearing regions were analyzed. The EDS spectra were dominated by the Ca peaks, with no other peaks appearing from possible impurities leached from the steel crucible. Light elements such as Li and C are not within the detection limits of this instrument. Therefore, additional elemental analysis was performed using a Perkin-Elmer Analyst 100 atomic absorption spectrophotometer to detect atomic emission of Li. A weighed sample of Ca_2LiC_3H (obtained from a Ca/Li/C/CaH_2 reaction ratio of 10:10:6:1) was dissolved in 2% aqueous HCl, and this solution was diluted to within the linear range of the detector. A quantitative calibration curve was obtained by serial dilution of a Li standard solution (1000 ± 1 ppm Li in 2% HCl, Fisher Chemicals). These solutions were ionized over an acetylene flame, and the lithium emission at 670.8 nm was measured. Comparison of the emission of the standard solutions to that of the sample indicated a Li content of 5.6% of the total mass of the sample (5.59% Li expected for the Ca_2LiC_3H stoichiometry). Analyses of carbon and hydrogen on a similarly synthesized sample were carried out by Atlantic Microlab Inc. (Theor. Calcd.: C, 29.03%; H, 0.81%. Found: C, 27.30%; H, 0.75%). While the carbon and hydrogen amounts are slightly lower than calculated (possibly due to flux coating or slight decomposition of the sample during transport), the 3:1 C:H ratio is in agreement with the stoichiometry Ca_2LiC_3H.

Thermal Analysis and Protolysis Study. The thermal stability of Ca_2LiC_3H was studied using a TA Instruments Q600 SDT Simultaneous DSC-TGA system. A large single crystal was placed in an alumina sample pan and heated to 1273 K at 10°/min under flowing argon to observe any phase transitions or decomposition. The reaction between Ca_2LiC_3H and NH_4Cl was carried out in a 100 mL flask sealed with a rubber septum to allow aliquots of gaseous products to be taken by syringe. Ca_2LiC_3H (0.124 g) and NH_4Cl (0.214 g, 99.5% Sigma-Aldrich) were added to the reaction flask inside the glovebox. The reaction flask was evacuated and then backfilled with nitrogen. The mixture of two powders was heated under flowing nitrogen to ∼470 K using a heating mantle. Gaseous aliquots were analyzed by injecting them into a HP6890 series GC system coupled to a Hewlett-Packard 5973 mass selective detector.

Table 1. Single-Crystal X-ray Diffraction Data Collection and Structural Refinement Parameters for Ca_2LiC_3H and CaH_2[a]

composition	Ca_2LiC_3H	CaH_2
formula weight (g/mol)	124.14	42.10
crystal system	tetragonal	orthorhombic
space group	*P4/mbm* (No. 127)	*Pnma* (No. 62)
collection temperature (K)	150	150
cell parameters (Å)	$a = 6.8236(1)$ $c = 3.7518(1)$	$a = 5.996(1)$ $b = 3.6022(8)$ $c = 6.834(1)$
V (Å^3)	174.69(1)	146.95(5)
Z	2	4
density, calc. (g/cm^3)	2.36	1.90
μ (mm^{-1})	3.0	3.5
data collection range (deg)	$4.22 < \theta < 47.29$	$4.23 < \theta < 28.16$
reflections collected	3191	1655
independent reflections	475 [$R_{int} = 0.0181$]	198 [$R_{int} = 0.0390$]
parameters refined	16	13
R_1[b]	0.0151	0.0211
wR_2[c] [$F_o > 4\sigma F_o$]	0.0407	0.0530
R_1, wR_2 (all data)	0.0165, 0.0407	0.0212, 0.0530
largest diff. peak and hole (e/Å^3)	0.59 and −0.36	0.52 and −0.62
GOF	1.149	1.215

[a] Further details of the crystal structure determination may be obtained from Fachinformationszentrum Karlsruhe, D-76344 Eggenstein-Leopoldshafen, Germany, on quoting the depository numbers CSD-421103 and CSD-421100 for Ca_2LiC_3H and CaH_2, respectively. [b] $R_1 = \sum||F_o| - |F_c||/\sum|F_o|$. [c] $wR_2 = [\sum w(F_o^2 - F_c^2)^2/\sum w(F_o^2)^2]^{1/2}$, $w = [\sum^2(F_o^2) + (A\cdot p)^2 + B\cdot p]^{-1}$; $p = (F_o^2 + 2F_c^2)/3$; $A = 0.0226$ (Ca_2LiC_3H), 0.022800 (CaH_2).

X-ray Diffraction. Sample crystals were brought out of the glovebox under Paratone oil. Small spheroid pieces cleaved from the larger bulk crystals were mounted in a cryoloop. Single-crystal X-ray diffraction data were collected at 150 K in a stream of nitrogen using a Bruker APEX 2 CCD diffractometer with a Mo Kα radiation source. Processing of the data was accomplished with use of the program SAINT; an absorption correction was applied to the data using the SADABS program.[9] Refinement of the structure was performed using the SHELXTL package.[10] The structure was solved in tetragonal space group *P4/mbm* (No. 127); crystallographic data can be found in Tables 1−3. During the structural refinement, Ca, Li, and C positions were determined, resulting in a reasonable Ca_2LiC_3 structure with suitable bond lengths and an *R*-value of 0.0162. However, an additional electron density peak was indicated in an octahedrally coordinated site defined by two Li and four Ca atoms (see Supporting Information, Figure S1). Assigning this peak as hydrogen led to an *R*-value of 0.0151. This atom was refined isotropically. Powder X-ray diffraction studies were carried out on reaction products to identify byproducts and to observe the effects of changing reaction stoichiometry. In a glovebox, samples of solid products from each reaction were ground with a small amount of LaB_6 as an internal standard and placed in an airtight sample holder. Data were collected using an original diffraction setup based on a Huber imaging plate

(8) (a) Fjellvag, H.; Karen, P. *Inorg. Chem.* **1992**, *31*, 3260–3263. (b) Karen, P.; Fjellvag, H. *J. Alloys Compd.* **1992**, *178*, 285–295. (c) Disch, S.; Cheetham, A. K.; Ruschewitz, U. *Inorg. Chem.* **2008**, *47*, 969–973.

(9) *SAINT, Version 6.02a*; Bruker AXS, Inc.: Madison, WI, 2000.

(10) Sheldrick, G. M. *SHELXTL NT/2000, Version 6.1*; Bruker AXS, Inc.: Madison, WI, 2000.

Table 2. Atomic Coordinates and Thermal Displacement Parameters for Ca_2LiC_3H and CaH_2[a]

atom	Wyckoff site	x/a	y/b	z/c	U_{eq}[b]
			Ca_2LiC_3H		
Ca(1)	4*h*	0.18142(2)	0.68142(2)	1/2	0.00552(4)
C(1)	4*g*	0.63735(9)	0.13735(9)	0	0.0085(1)
C(2)	2*d*	0	1/2	0	0.0055(1)
Li(1)	2*a*	0	0	0	0.0181(5)
H(1)	2*b*	0	0	1/2	0.017(7)[c]
			CaH_2		
Ca(1)	4*c*	0.26043(5)	1/4	0.39014(5)	0.0058(2)
H(1)	4*c*	0.029(3)	1/4	0.672(3)	0.021(4)[c]
H(2)	4*c*	0.138(3)	1/4	0.072(2)	0.028(5)[c]

[a] All site occupancies are 100%. [b] U_{eq} is defined as one-third of the trace of the orthogonalized U_{ij} tensor. [c] Isotropic refinement.

Table 3. Selected Interatomic Distances (Å) in the Ca_2LiC_3H Structure

bond	distance, Å
Ca(1)−C(1)	2.5647(6) × 2
Ca(1)−C(1)	2.8880(4) × 4
Ca(1)−C(2)	2.5659(1) × 2
Ca(1)−Li(1)	3.1269(1) × 4
C(1)−C(2)	1.3254(9) × 2
C(1)−Li(1)	2.6461(4) × 2
Li(1)−H(1)	1.8759(1) × 2
Ca(1)−H(1)	2.5016(1) × 4

Guinier camera 670 using Cu Kα_1 radiation (λ = 1.54060 Å) with Ge crystal monochromator. X-ray patterns were acquired at 0.005° resolution at ambient temperature. During the data collection, the sample was placed in an evacuated sample holder to prevent oxidation. The JADE software suite was used for analysis of the powder patterns.

NMR Spectroscopy. Magic angle spinning (MAS) ^{7}Li, ^{1}H, and ^{13}C NMR data were collected on a Varian Inova 500 wide-bore spectrometer at room temperature. LiCl powder was used as external reference for ^{7}Li and tetramethylsilane (TMS) for ^{1}H and ^{13}C. For the ^{7}Li NMR study, samples of solid product from several Ca/Li/C/CaH_2 reactions of differing stoichiometries were each ground with KBr in a drybox (1:4 sample to KBr ratio by mass) to facilitate spinning of the sample in the magnetic field; the mixtures were packed into 2.5 mm zirconia rotors with airtight screw caps. ^{7}Li NMR data were collected at 25 °C and a 13−15 kHz spin rate. A one-pulse sequence was used with a pulse width of 5 μs and a recycle delay of 15 μs. A total of 400 scans were collected for each spectrum. For the ^{13}C and ^{1}H MAS NMR experiments, only the product from a Ca/Li/C/CaH_2 flux reaction of ratio 10:10:6:1 was analyzed. The ^{13}C spectrum (Figure S2, Supporting Information) was collected on a sample in a 4 mm rotor spinning at 4 kHz with a pulse width of 4 us and a recycle delay of 300 s; 800 pulses were totaled. The spectrum was fitted using Origin software. The ^{1}H spectrum (Figure S3, Supporting Information) was collected for a sample in a 4 mm rotor spinning at 8 kHz. The ^{1}H spectrum is the sum of 1600 pulses, each with a pulse width of 5 μs and a recycle delay of 1 s.

Quantum Chemical Calculations. Calculations of density of states (DOS) were performed with the tight binding-linear muffin tin orbitals-atomic sphere approximation TB-LMTO-ASA program package,[11a] based on the experimentally determined unit cell dimensions and atomic coordinates for Ca_2LiC_3H. For comparison, the same type of calculations were performed for the hypothetical nonhydride version, Ca_2LiC_3, and on the related phase Mg_2C_3. The structural parameters for Mg_2C_3 were taken from published data.[8a]

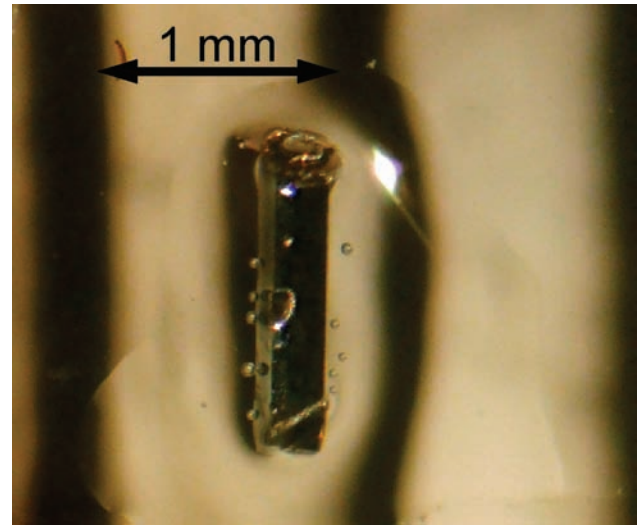

Figure 1. A crystal of Ca_2LiC_3H under Paratone oil.

The radial scalar-relativistic Dirac equation was solved to obtain the partial waves. Interstitial empty spheres were added to fill the interstitial space in the case of Ca_2LiC_3 (r(E1) = 1.00 Å and r(E2) = 1.02 Å) and Mg_2C_3 (1.1 Å ≤ r(E) ≤ 1.66 Å), while for Ca_2LiC_3H no empty spheres had to be added. The calculation was made for 1056 κ points in the irreducible Brillouin zone in the case of Ca_2LiC_3H and Ca_2LiC_3 and for 1936 κ points in the case of Mg_2C_3. Integration over the Brillouin zone was made by the tetrahedron method.[11b] The following radii of atomic spheres were applied for the calculations: for Ca_2LiC_3H, r(Ca) = 3.78 Å, r(Li) = 2.74 Å, r(H) = 1.35 Å, r(C) = 1.45 Å; for Ca_2LiC_3, r(Ca) = 3.50 Å, r(Li) = 3.34 Å, r(C) = 1.45 Å; for Mg_2C_3, r(Mg) = 3.16 Å, r(C) = 1.46 Å. The basis sets contained Ca(3s, 3d), Li(2s), H(1s), Mg(2s, 2p), and C(2s, 2p) with Ca(3p), Li(2p, 3d), H(2p, 3d), Mg(3d), and C(3d) functions being downfolded.

Electron localization function, ELF, η, was calculated on an adequately fine mesh of 0.03−0.04 Å.[12] The Data Explorer program was used for visualization of ELF isosurfaces.[13] The topology of ELF and calculation of basin populations was carried out using the program Basin implemented into DGrid v.4.4.[14]

Results and Discussion

Synthesis. Ca_2LiC_3H grows in a 1:1 Ca/Li melt as silvery, reflective, rod-like crystals and agglomerates. Individual crystals up to 1 mm in length are obtained; see Figure 1. This phase is unstable to moisture and air and was therefore stored and handled under argon. When heated under argon, the phase is stable to 950 K, at which point it decomposes with a rapid weight loss. The highest yield is produced from a Ca/Li/C/CaH_2 ratio of 10:10:6:1; the yield is approximately 70% based on carbon. The title phase was initially synthesized in the absence of a hydrogen source. The adventitious hydrogen in Ca/Li/C reactions likely came from the calcium or lithium reactants. These metals were not distilled after purchase; even though they were stored in a glovebox, they can react with trace water to form metal hydroxides and hydrogen gas. The hydrogen gas

(11) (a) Jepsen, O.; Burkhardt, A.; Andersen, O. K. *The Program TB-LMTO-ASA, version 4.7*; Max-Planck-Institut für Festkörperforschung: Stuttgart, Germany, 2000. (b) Blöchl, P. E.; Jepsen, O.; Andersen, O. K. *Phys. Rev. B* **1994**, *49*, 16223–16233.

(12) (a) Becke, A. D.; Edgecombe, K. E. *J. Chem. Phys.* **1990**, *92*, 5397–5403. (b) Savin, A.; Becke, A. D.; Flad, J.; Nesper, R.; Preuss, H.; von Schnering, H. G. *Angew. Chem., Int. Ed. Engl.* **1991**, *30*, 409–412. (c) Savin, A.; Nesper, R.; Wengert, S.; Fässler, T. F. *Angew. Chem., Int. Ed. Engl.* **1997**, *36*, 1808–1832. (d) http://www.cpfs.mpg.de/ELF/index.php.

(13) *IBM's Open Visualization Data Explorer*, Version 4.4.4; http://www.opendx.org.

(14) Kohout, M. *DGrid, version 4.4*; Radebeul, Germany, 2008.

will then react with the metal to form metal hydride; as a result of this, commercial alkaline earth metals may contain up to 20 at. % hydrogen.[15] Extensive research by the Corbett group has indicated that inadvertent hydride incorporation is common in the synthesis of alkaline earth-rich phases; careful synthetic investigations on reported phases Ba_5Ga_6, $Ba_{21}Ge_2O_5$, and the A_5Sb_3 (A = Ca, Sr, Ba) family showed that these compounds are actually Zintl phase hydrides ($Ba_5Ga_6H_2$, $Ba_{21}Ge_2O_5H_{24}$, and A_5Sb_3H).[16−18] The yield of these phases is greatly improved when hydride is deliberately added.

After XRD structure refinement revealed the presence of the hydride anion in Ca_2LiC_3H (vide infra), calcium hydride was deliberately added to subsequent reactions. Ca/Li/C/CaH_2 ratios of 10:10:6:*x* (*x* = 0, 0.25, 0.5, 0.75, and 1.0) mmol were used. Powder diffraction of the samples (Figure S4, Supporting Information) indicates that calcium carbide and calcium hydride are formed as byproducts. CaC_2 is the main product in reactions with little or no CaH_2 added; the yield of Ca_2LiC_3H increases as larger amounts of CaH_2 reactant are used. Recrystallized CaH_2 becomes increasingly prevalent in reactions with large amounts of CaH_2. The CaH_2 crystals form as large (1−2 mm length) colorless transparent rods, easily distinguishable from the silver crystals of the title phase. The high quality of these crystals allowed for improved structural characterization for this compound, including refinement of the hydrogen positions. This information is of interest, because previous structural studies on CaH_2 have reported incorrect hydride positions or were carried out on powdered samples or on deuterides.[19] The crystallographic data for CaH_2 are therefore included in Table 1 and in the Supporting Information. Ca_2LiC_3H can also be made from a stoichiometric ratio of reactants, using a heating profile identical to the flux reactions. Product yield of stoichiometric reactions was roughly 30% and of poorer crystal quality than product obtained from flux; a significant amount of CaC_2 byproduct is apparent by powder X-ray analysis.

Structure. Ca_2LiC_3H crystallizes with a new structure type in tetragonal space group *P*4/*mbm*, shown in Figure 2. The refinement of the positions and occupancy of the non-hydrogen atoms was straightforward. All these sites are fully occupied; the calcium, lithium, and carbon positions correspond to the cesium, amide nitrogen, and azide positions in the $Cs_2(NH_2)N_3$ structure type, respectively.[20] However, an additional peak in the residual electron density of ∼1 e Å^3 became apparent in the final stages of the structural refinement; see Figure S1. This peak is consistently seen in the single-crystal X-ray diffraction analyses of crystals from several different Ca/Li/C/CaH_2 flux reactions. It is located on the 2*b* Wyckoff site, a site surrounded by 4 neighboring Ca atoms and 2 neighboring Li atoms; the actual observation of an electron density peak at this site was possible because of these relatively light neighboring atoms. The assignment of this peak as hydrogen was made on the basis of previous reports of adventitious hydride incorporation and from inspection of the bond distances to surrounding atoms. The Ca_2LiC_3H structure can therefore be viewed as a stuffed

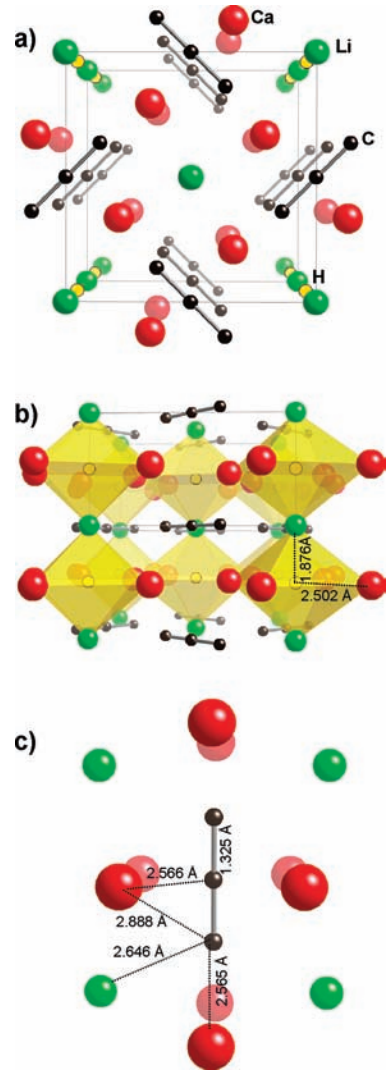

Figure 2. (a) Structure of Ca_2LiC_3H, viewed down the *c*-axis. (b) Structure viewed down the *a*-axis; octahedral sites of the hydride anions are highlighted in yellow. (c) Local environment of the C_3^{4-} anion.

variant of the $Cs_2(NH_2)N_3$ structure type. The Ca−H distance of 2.5016(1) Å is longer than the range of 2.30−2.36 Å for Ca−H in CaH_2; it is also longer than the sum of ionic radii for these elements (2.24 Å).[21] On the other hand, the 1.8759(1) Å distance from the hydride to the two adjacent Li ions is shorter than that in LiH (2.031 Å) and shorter than the sum of ionic radii (1.98 Å). Similarly short Li−H distances of 1.88 Å were reported for Li_4Si_2H; this strong bonding was surmised to stabilize the ternary hydride phase.[22]

The occupancy of the hydrogen site was fixed at 100% because it cannot be refined based on X-ray single-crystal data. The possibility of variable hydride content ($Ca_2LiC_3H_x$, with $0 < x < 1$) was considered; intermetallic hydrides allow for a wide range of hydrogen incorporation ($0 < x < 6$ for $LaNi_5H_x$, for example), and small deviations from unity are also reported in more charge-balanced systems such as $Ca_5Bi_3H_x$.[23] However, powder and single-crystal diffraction of products of reactions

(15) Peterson, D. T. *J. Met.* **1987**, *39*, 20–23.
(16) Henning, R. W.; Leon-Escamilla, E. A.; Zhao, J. T.; Corbett, J. D. *Inorg. Chem.* **1997**, *36*, 1282–1285.
(17) Huang, B. Q.; Corbett, J. D. *Inorg. Chem.* **1998**, *37*, 1892–1899.
(18) Leon-Escamilla, E. A.; Corbett, J. D. *J. Alloys Compd.* **1998**, *265*, 104–114.
(19) (a) Alonso, J. A.; Retuerto, M.; Sanchez-Benitez, J.; Fernandez-Diaz, M. T. *Z. Kristallogr.* **2010**, *225*, 225–229. (b) Zintl, E.; Harder, A. *Z. Elektrochem.* **1935**, *41*, 33–52.
(20) Harbrecht, B.; Jacobs, H. *Z. Anorg. Allg. Chem.* **1983**, *500*, 181–187.
(21) Shannon, R. D. *Acta Crystallogr., Sect. A* **1976**, *32*, 751–767.
(22) Wu, H.; Zhou, W.; Udovic, T. J.; Rush, J. J.; Yildirim, T.; Hartman, M. R.; Bowman, R. C.; Vajo, J. J. *Phys. Rev. B* **2007**, *76*, 224301.
(23) Leon-Escamilla, E. A.; Dervenagas, P.; Stassis, C.; Corbett, J. D. *J. Solid State Chem.* **2010**, *183*, 114–119.

carried out with differing amounts of CaH_2 showed none of the variation in unit cell parameters which is typically associated with Vegard's law behavior. Instead, the unit cell parameters remained constant, but the yield and product quality of the title phase improved as the amount of CaH_2 reactant was increased. This indicates that this phase forms in the completely hydrided state, which is also properly charge-balanced.

The title compound is one of a very small number of inorganic compounds containing the C_3^{4-} anion. This chain of three carbons, which can be viewed as deprotonated propadiene (C_3H_4, also known as allene), is also found in Mg_2C_3, Sc_3C_4, R_4C_7 (R = Y, Ho, Er, Tm, Lu), $R_5Re_2C_7$ (R = Sc, Er, Tm, Lu), and $Ca_3C_3Cl_2$.[6,8,24−26] In Ca_2LiC_3H, this anion is perfectly linear, with the central carbon located on a center of inversion. The C−C bond length of 1.3254(9) Å is similar to that in propadiene (∼1.31 Å), indicating its double bond nature; the other reported structures containing the C_3^{4-} unit also feature a C−C bond of similar length (range: 1.32−1.35 Å). The distribution of cations around this unit is shown in Figure 2c. While Mg_2C_3 and Sc_3C_4 both feature clustering of cations around the terminal carbons of the C_3^{4-} anion (in agreement with the location of formal charges), Ca_2LiC_3H, R_4C_7, and $Ca_3C_3Cl_2$ have short metal−carbon bonds to the central carbon as well. This may be indicative of the relative ionicity of the interactions between the metal cations and the C_3^{4-} unit, with the smaller and more polarizing Mg^{2+} and Sc^{3+} inducing a more covalent interaction with the terminal carbon atoms of the carbide anion, as compared to the more ionic interactions with larger cations Ca^{2+} and R^{3+}. This is also indicated by electron localization function analysis (vide infra).

Reaction of a compound containing the C_3^{4-} unit with a protic reagent should yield gaseous C_3H_4, as was reported for Mg_2C_3 and R_4C_7.[8,24] Ca_2LiC_3H reacts rapidly and violently with water. A more controllable protolysis reaction was carried out using ammonium chloride as the source of acidic protons via its thermal decomposition to gaseous HCl and ammonia, following the procedure of a similar study on Mg_2C_3.[8] The reaction with Ca_2LiC_3H is shown below:

$$Ca_2LiC_3H\,(s) + 5NH_4Cl\,(s) \rightarrow 2CaCl_2\,(s) + LiCl\,(s) + 5NH_3\,(g) + C_3H_4\,(g) + H_2\,(g)$$

The mass spectra of aliquots of gaseous products feature a strong signal at 39 *m*/*z*, confirming production of C_3H_4. This could be in the form of propadiene or propyne or a mixture of these isomers (this was seen for the protolysis of Mg_2C_3), although the envelope of isotopes from *m*/*z* = 35−40 better matches that of propadiene.[27] Both gases are of interest for industrial uses (as gas welding fuels, either pure or in a methyl acetylene−propadiene−propane mixture known as MAPP gas), and they are also convenient building blocks for organic synthesis. The reaction of elemental carbon to form Ca_2LiC_3H and the ready protolysis of this phase to form C_3H_4 may be a valuable method to convert carbon into useful multiple bonded reactants for organic syntheses or to produce isotopically enriched precursors.[28] Mg_2C_3 is also of interest for this. However, synthesis of this compound involves reaction of Mg powder with flowing pentane gas at high temperatures, or lengthy (85 h) ball milling of the elements followed by annealing; both syntheses are somewhat inconvenient.[8,28]

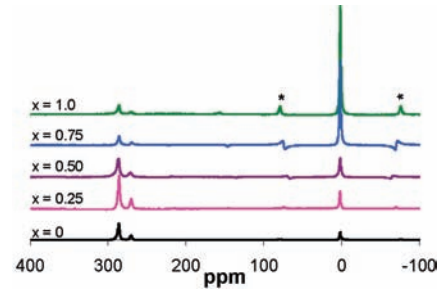

Figure 3. ^{7}Li MAS NMR spectra of Ca_2LiC_3H samples synthesized using Ca/Li/C/CaH_2 mmol ratios of 10:10:6:*x*. Spinning sidebands are marked with asterisks.

With the incorporation and full occupancy of the H^- and C_3^{4-} anions, the title phase has a charge-balanced composition, $(Ca^{2+})_2Li^+(C_3)^{4-}(H^-)$. This appears to be the only reported structure with ordered coexisting carbide and hydride anions. A number of studies have been carried out on rare earth carbide hydrides such as $YbC_{0.5}H$ and $La_2C_3H_{1.5}$, but these are highly disordered (and in the latter case amorphous) phases with varying amounts of interstitial carbon and hydrogen.[29,30] The most comparable compound is $La_2C_2H_2$, which forms from the reaction of La_2C_3 with hydrogen at 1070K. It is theorized to contain both interstitial H^- (in tetrahedral sites) and C_2^{4-} units (in octahedral sites), but was characterized by powder diffraction, and actual refinement of the structure from the powder data was not possible (XRD data were dominated by La scattering; the approximate structure model is based on $La_2C_2O_2$).[31]

NMR Spectroscopy. ^{7}Li MAS NMR data were collected at room temperature for products of reactions of Ca/Li/C/CaH_2 in mmol ratios of 10:10:6:*x*, with *x* = 0, 0.25, 0.5, 0.75, and 1 mmol. All spectra in Figure 3 exhibit the same three lithium resonances: two in the Knight-shifted metallic lithium region (286 and 270 ppm) and one in the ionic lithium region (4 ppm, referenced to LiCl). As the amount of CaH_2 reactant increases, the intensity of the ionic lithium peak in the product spectrum increases. This is in accordance with the increasing yield of Ca_2LiC_3H, indicating that this peak at 4 ppm corresponds to the lithium in this phase. The two metallic lithium peaks at 286 and 270 ppm always occur at a 3:1 ratio. They are likely due to $CaLi_2$; this intermetallic will be formed in the solidified residual traces of Ca/Li flux adhering to the solid products after centrifugation. Weak peaks in the powder XRD patterns for these samples indicate the presence of this phase. $CaLi_2$ has the C14 Laves phase structure (hexagonal space group $P6_3/mmc$), with lithium atoms in 2*a* and 6*h* Wyckoff sites.[32] The

(24) (a) Mattausch, H.; Gulden, T.; Kremer, R. K.; Horakh, J.; Simon, A. *Z. Naturforsch., B* **1994**, *49*, 1439–1443. (b) Czekalla, R.; Jeitschko, W.; Hoffmann, R. D.; Rabeneck, H. *Z. Naturforsch., B* **1996**, *51*, 646–654.
(25) (a) Pöttgen, R.; Jeitschko, W. *Z. Naturforsch., B* **1992**, *47*, 358–364. (b) Pöttgen, R.; Wachtmann, K. H.; Jeitschko, W.; Lang, A.; Ebel, T. *Z. Naturforsch., B* **1997**, *52*, 231–236.
(26) (a) Hoffmann, R.; Meyer, H. J. *Z. Anorg. Allg. Chem.* **1992**, *607*, 57–71. (b) Meyer, H. J. *Z. Anorg. Allg. Chem.* **1991**, *593*, 185–192.
(27) Stein, S. E. Mass Spectra. In *NIST Chemistry WebBook, NIST Standard Reference Database Number 69*; Linstrom, P. J., Mallard, W. G., Eds.; National Institute of Standards and Technology: Gaithersburg, MD, 2008; http://webbook.nist.gov.
(28) Hick, S. M.; Griebel, C.; Blair, R. G. *Inorg. Chem.* **2009**, *48*, 2333–2338.
(29) Haschke, J. M. *Inorg. Chem.* **1975**, *14*, 779–783.
(30) Kienle, L.; Garcia Garcia, F. J.; Duppel, V.; Simon, A. *J. Solid State Chem.* **2006**, *179*, 993–1002.
(31) Simon, A.; Gulden, T. *Z. Anorg. Allg. Chem.* **2004**, *630*, 2191–2198.
(32) Villars, P.; Calvert, L. D. *Pearson's Handbook−Crystallographic Data for Intermetallic Phases*; ASM International: Materials Park, OH, 1998.

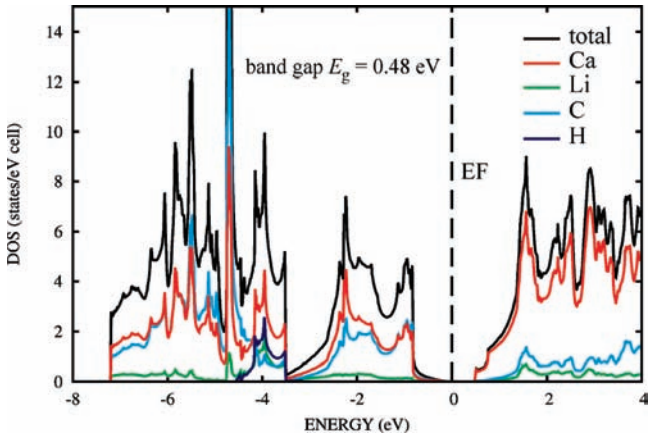

Figure 4. Total and partial density of states for Ca_2LiC_3H. Contributions from Ca, Li, C, and H are color-coded.

two lithium sites are in the proper ratio to consistently produce NMR peaks in a 3:1 ratio, and their Knight shifted resonances (close to the 290 ppm for elemental lithium) are in agreement with the metallic nature of this compound.

The ^{13}C MAS NMR spectrum of Ca_2LiC_3H (Figure S2) exhibits a broad asymmetric peak, which can be deconvoluted into a large peak at 126 ppm and a smaller peak at 225 ppm, in a roughly 2:1 ratio. This is in agreement with the two crystallographic carbon sites and their associated multiplicity (terminal carbon atoms on 4*g* sites and the central carbon atom on a 2*d* site). Molecular allene exhibits resonances at 74.8 ppm (terminal carbons) and 213.5 ppm (central carbon).[33] The carbon resonances of the anionic C_3^{4-} are expected to be shifted downfield; similar shifting is seen for the ^{13}C resonance of metal acetylides when compared to that of acetylene.[34]

Ca_2LiC_3H exhibits only one very broad peak in its ^1H MAS NMR spectrum, at approximately 3 ppm (Figure S3). The majority of reported ^1H shifts for alkaline earth hydrides are more negative; shifts of −4.5, −6.7, and −8.7 ppm are seen for CaH_2, SrH_2, and BaH_2, respectively.[35] Complex hydrides with an H^- anion surrounded by alkaline earth cations also commonly exhibit negative ^1H shifts, as seen for Ba_5Sb_3H (−8.5 ppm) and Ba_9In_4H (−9.0 ppm).[36,37] The ^1H shift of +3 ppm indicates that the hydrogen nuclei of Ca_2LiC_3H are deshielded as compared to typical metal hydrides, possibly due to polarization of the electrons by the neighboring Li^+ cations. It is notable that LiH, MgH_2, and AlH_3, phases with considerable polarization and covalence in their metal−hydrogen interactions, also have ^1H resonances around 3 ppm.[38]

Electronic Calculations. The density of states (DOS) diagram for Ca_2LiC_3H is shown in Figure 4. In agreement with its charge-balanced stoichiometry, the compound is a semiconductor with a small band gap (E_g = 0.48 eV). Because of the air sensitivity

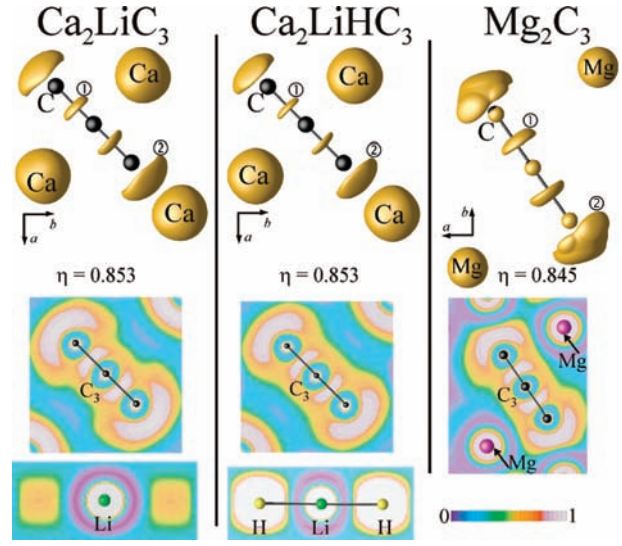

Figure 5. 3-D isosurfaces of electron localization function (η) at selected values of η (top row) for hypothetical Ca_2LiC_3 (left column), Ca_2LiC_3H (middle), and Mg_2C_3 (right). Localization domain 1 corresponds to the C═C bond within the linear C_3-unit, and domain 2 indicates the lone pairs of terminal C atoms. 2-D contour plots (color bar in lower right corner) are shown of the η distribution around the C_3 anion (middle row) and H−Li−H unit (bottom row).

of this phase, diffuse reflectance spectroscopy and resistivity measurements could not be carried out to confirm the band gap. However, the silver color and reflectance indicates the band gap is below 1 eV. The hydride bands are narrow and largely localized at around −4 eV below the Fermi level; the lithium-derived states are also found in this energy range. Similar localization and hybridization between Li and H states was reported for Li_4Si_2H.[22] Both phases also feature short Li−H bonds as compared to the sum of their ionic radii; strong Li−H interactions may act to stabilize these phases. The states just below E_f are dominated by contributions from carbon p-orbitals and calcium d-orbitals.

The chemical bonding in Ca_2LiC_3H was analyzed by means of electron localization function (ELF, η), which is a quantum-mechanical tool used to examine the chemical bonding in direct space. The topological analysis of ELF highlights the presence of localization domains, which correspond to atomic shells, chemical bonds, and lone electron pairs.[12] There are three types of localization domains in the title phase, shown in Figure 5: core domains, domain ① corresponding to the homonuclear covalent bonds between carbon atoms within the linear C_3-unit, and domain ② indicating the lone pairs of terminal carbon atoms. No additional domains corresponding to covalent interactions between Li−C or Ca−C were found. Thus, the chemical bonding coincides with a classical picture of a covalently bonded C_3^{4-} unit, which has ionic interactions with neighboring cations.

A very powerful aspect of ELF analysis is its ability to determine the preferred positions of hydrides if they cannot be located using X-ray crystallography studies. For example, the ELF analysis of the Ca substructure in CaH_2 reveals ELF-maxima, which correspond to the positions of H^-.[12c] To explore this capability, ELF was calculated for both the Ca_2LiC_3 and the Ca_2LiC_3H structures. Our calculations for hydrogen-free Ca_2LiC_3 revealed additional ELF maxima in between Li atoms, that is, in the position of the H^- in the hydrided compound Ca_2LiC_3H (Figure 5, bottom left). The integration of the basin corresponding to this domain yields a value close to 1 (Table

(33) Beeler, A. J.; Orendt, A. M.; Grant, D. M.; Cutts, P. W.; Michl, J.; Zilm, K. W.; Downing, J. W.; Facelli, J. C.; Schindler, M. S.; Kutzelnigg, W. *J. Am. Chem. Soc.* **1984**, *106*, 7672–7676.
(34) Ruschewitz, U. *Coord. Chem. Rev.* **2003**, *244*, 115–136.
(35) Nicol, A. T.; Vaughan, R. W. *J. Chem. Phys.* **1978**, *69*, 5211–5213.
(36) Boss, M.; Petri, D.; Pickhard, F.; Zönnchen, P.; Röhr, C. *Z. Anorg. Allg. Chem.* **2005**, *631*, 1181.
(37) Wendorff, M.; Scherer, H.; Röhr, C. *Z. Anorg. Allg. Chem.* **2010**, *636*, 1038–1044.
(38) (a) Hwang, S. J.; Bowman, R. C.; Graetz, J.; Reilly, J. J. *Mater. Res. Soc. Symp. Proc.* **2006**, *927*, 0927-EE03−03. (b) Magusin, P. C. M. M.; Kalisvaart, W. P.; Notten, P. H. L.; van Santen, R. A. *Chem. Phys. Lett.* **2008**, *456*, 55–58. (c) Bowman, R. C.; Hwang, S. J.; Ahn, C. C.; Vajo, J. J. *Mater. Res. Soc. Symp. Proc.* **2005**, *837*, N3.6.1.

Table 4. Results of Integration of Electron Localization Basins for Ca_2LiC_3, Ca_2LiC_3H, and Mg_2C_3

	basin population, q/e		
atom, feature	Ca_2LiC_3	Ca_2LiC_3H	Mg_2C_3
core: Ca or Mg	18.46 × 2	18.46 × 2	10.12 × 2
core: Li	2.06	2.04	
core: C	2.13 × 3	2.11 × 3	2.13 × 3
core: H		1.94	
terminal lone pair: C	4.52 × 2	4.39 × 2	4.55 × 2
bond: C═C	2.91 × 2	3.04 × 2	3.10 × 2
ELF maxima[a]	0.78		
sum	61.01	62.09	41.93
theoretical sum	61	62	42

[a] ELF maxima located between two Li atoms, corresponding to the hydrogen position in Ca_2LiC_3H.

4). This is further indication of the stabilization due to hydride incorporation in the crystal structure. The shape of the ELF maxima corresponding to the H position is similar to that in CaH_2. The results of ELF analysis of the Ca_2LiC_3H structure are also shown in Figure 5. The values of the lithium and hydride ion basin populations coincide with the ionic species Li^+ and H^-; similar values are found for the basin populations in lithium hydride LiH.[39] The Li^+ and H^- ions in Ca_2LiC_3H are strongly polarized, which is reflected by deviations from the spherical symmetry of the core domains, especially in the case of H^-. This is in agreement with the DOS calculations and ^1H NMR data and is further indication of a strong stabilizing interaction.

ELF analysis also sheds light on the nature of the C_3^{4-} anion in this structure. For the determination of the bond order between carbon atoms, the integration of the basins corresponding to the core, bonds, and lone pair was performed for Ca_2LiC_3H and for the hydride-free composition Ca_2LiC_3 for comparison (Table 4). For simple molecules such as $H_3C{-}CH_3$, $H_2C{=}CH_2$ or $HC{\equiv}CH_3$, the integration of the basin corresponding to the C−C bond results in electronic basin populations of 1.83 e−, 3.52 e−, and 5.27 e−, which agrees fairly well with the expected number of electrons in single, double, and triple C−C bonds, respectively.[40] However, for Ca_2LiC_3 and Ca_2LiC_3H, the integration resulted in values of 2.9 and 3.0 e−, respectively. This inconsistency may stem from different degrees of electron localization in the ionic solid versus the molecular state. It was shown recently that a suitable reference system should be used for the calculation of the effective bond order.[41] For instance, CaC_2 could be used as a prototype of the triple C≡C bond in ionic solids featuring the C_2^{2-} anion. We have chosen Mg_2C_3 as a reference for the C═C double bond within the linear C_3^{4-} unit. Its crystal structure features linear C_3 units similar to those in Ca_2LiC_3H, and both Mg_2C_3 and Ca_2LiC_3H yield C_3H_4 from protolysis reactions. The ELF diagrams for Mg_2C_3 are shown in Figure 5. It is notable that instead of one localization domain corresponding to the lone pair on the terminal carbon atom, there are three distinctive domains in Mg_2C_3, which are clearly separated at values of $\eta > 0.85$. This reflects the stronger covalency of the Mg−C contacts as compared to the Ca−C interactions in Ca_2LiC_3H. Using Mg_2C_3 as a reference for the double bond within the C_3 linear unit, the effective bond order for the C═C bond in Ca_2LiC_3H is calculated as follows: $(n_{C=C}) \times (Ca_2LiC_3H/Mg_2C_3) = (2) \times (3.0/3.1) = 1.9$, which is fairly close to 2, indicating a double bond.[42] Thus, the C═C bonds within C_3 units in Ca_2LiC_3H are similar to the double bonds in Mg_2C_3. The total number of electrons for the C_3^{4-} unit in Ca_2LiC_3H is calculated as [3 × 2.11 e− (C core)] + [2 × 4.39 e− (C lone pair)] + [2 × 3.04 e− (C═C bonds)] = 21.19 e−. This is smaller than the theoretically expected 22 e− for a C_3^{4-} unit. This difference is not due to errors of integration, but is instead a chemical bonding effect known from atomic shell structure studies.[43] Similar values are obtained for the C_3^{4-} unit in the hypothetical Ca_2LiC_3.

Ca_2LiC_3H occupies a gray area of materials classification. It can be viewed as a complex salt or potentially as a Zintl phase. The salt-like nature of this compound is evident in the stoichiometry and ELF analysis and in its similarities to Mg_2C_3. The analogous Ca_2C_3 does not exist; reactions of calcium and carbon produce only the acetylide CaC_2 or graphite intercalation compounds. The title phase can be viewed as a double salt $[Ca_2C_3][LiH]$, in which the presence of LiH chains running along the *c*-axis stabilizes the Ca_2C_3 units. On the other hand, the small band gap supports the classification of Ca_2LiC_3H as a Zintl phase. Zintl phases are most narrowly defined as compounds derived from the reaction of electropositive metals (groups 1 and 2) with main group metalloid elements. Electron transfer from the metal reduces the metalloid element(s), which bond together to achieve a stable octet electron configuration, forming polyanionic clusters, layers, or frameworks.[44] This electron transfer results in a closed shell configuration and semiconducting properties; the presence of main group polyanions leads to small bandgaps, usually below 2 eV. Hydrogen can be incorporated into Zintl phases as isolated hydrides (exemplified by the title phase).[5] Zintl phases hydrides featuring the heavier group 14 (tetrelide, Tt) elements have been reported previously. Silicon and germanium form Li_4Tt_2H, featuring anionic zigzag chains of tetrelide separated by layers of hydride-centered Li octahedra.[22] Tin and lead both form the Ca_3TtH_2 Zintl phase, in which the tetrelide occurs as an isolated Tt^{4-} anion.[45] Of the Zintl phases featuring isolated hydride anions, Ca_2LiC_3H is unique in its incorporation of carbon as the metalloid, and the presence of multiple bonding in the polyanion.

Conclusions

Molten calcium/lithium mixtures are proving to be very fruitful synthesis media for new intermetallic and complex salt phases. The reaction of carbon and CaH_2 in this flux yields Ca_2LiC_3H, featuring C_3^{4-} and H^- anions. The interaction of lithium with the hydride anion appears to be of particular importance for stabilizing this compound. Reactions of other elements with CaH_2 in Ca/Li flux are now being explored to seek new hydride phases; recent products include $Ca_7LiSi_3H_3$. In addition to possessing new structure types, these compounds may be of interest for hydrogen storage.

(39) Bronger, W.; Kniep, R.; Kohout, M. *Z. Anorg. Allg. Chem.* **2005**, *631*, 265–271.
(40) (a) Ponec, R.; Chaves, J. *J. Comput. Chem.* **2005**, *26*, 1205–1213. (b) Noury, S.; Colonna, F.; Savin, A.; Silvi, B. *J. Mol. Struct.* **1998**, *450*, 59–68. (c) Chesnut, D. B. *Chem. Phys.* **2001**, *271*, 9–16.
(41) (a) Afyon, S.; Höhn, P.; Armbrüster, M.; Baranov, A.; Wagner, F. R.; Somer, M.; Kniep, R. *Z. Anorg. Allg. Chem.* **2006**, *632*, 1671–1680. (b) Dashjav, E.; Prots, Y.; Kreiner, G.; Schnelle, W.; Wagner, F. R.; Kniep, R. *J. Solid State Chem.* **2008**, *181*, 3121–3130.
(42) For the purpose of comparison, to determine the electronic basin population of the lone pair in the case of Mg_2C_3, the values for three domains were summed. The bond order of C═C bond in Ca_2LiC_3H with Mg_2C_3 as a reference was calculated as follows: $n_{C=C}$ (Ca_2LiC_3H/Mg_2C_3) = 3.0 (basin population of C═C bond in Ca_2LiC_3H) × 2 (assumed bond order for the double bond)/3.1 (basin population of C═C bond in Mg_2C_3) = 1.9.
(43) Kohout, M.; Savin, A. *Int. J. Quantum Chem.* **1996**, *60*, 875–882.
(44) Kauzlarich, S. M., Ed. *Chemistry, Structure, and Bonding of Zintl Phases and Ions*; VCH: Weinheim, 1996.
(45) Huang, B.; Corbett, J. D. *Inorg. Chem.* **1997**, *36*, 3730–3734.

Acknowledgment. This research was supported by the National Science Foundation under grant award number DMR-05-47791, and by the FSU Department of Chemistry and Biochemistry. We thank Dr. Umesh Goli for assistance with the mass spectrometry, Dr. Haidong Zhou at NHMFL for assistance with the powder diffraction studies, and Prof. Frank Haarmann (RWTH Aachen University) for useful discussion. This research made use of the NMR Facility of the FSU Department of Chemistry and Biochemistry and the scanning electron microscope facilities of the FSU Physics Department.

Supporting Information Available: Crystallographic data for Ca_2LiC_3H and CaH_2 in the form of CIF files. Residual electron density map for Ca_2LiC_3. ^{13}C and ^{1}H MAS NMR spectra for Ca_2LiC_3H. X-ray powder diffraction patterns for Ca_2LiC_3H samples. Density of states diagram for nonhydrided Ca_2LiC_3. This material is available free of charge via the Internet at http://pubs.acs.org.

JA107436N